

Electronic Supplementary Information (ESI) for

**Multifunctional chemical sensors and luminescent thermometers
based on Lanthanide metal-organic framework materials**

Kai-Min Wang,^a Lin Du,^a Yu-Lu Ma,^a Jing-Song Zhao,^a Quan Wang,^a Tong Yan,^a and Qi-Hua Zhao^{*a}

a. *Key Laboratory of Medicinal Chemistry for Natural Resource Education Ministry, School of Chemical Science and Technology, Yunnan University, Kunming, 650091, P. R. China.* ;

E-mail: qhzhao@ynu.edu.cn .

Experimental Section

General information: All of the reagents and solvents used in reactions were purchased from Adamas-beta Corporation Limited and used without purification, unless otherwise indicated. The NMR spectra were recorded on a Bruker DRX400 (¹H: 400 MHz, ¹³C: 100 MHz), chemical shifts (δ) are expressed in ppm, and *J* values are given in Hz, and deuterated DMSO was used as solvent. IR spectra were recorded on a FT-IR Thermo Nicolet Avatar 360 using KBr pellet. All Powder X-ray diffraction (PXRD) analyses were recorded on a Rigaku Dmax2500 diffractometer with Cu K α radiation ($\lambda = 1.54056 \text{ \AA}$). Thermal stability studies were carried out on a NETSCH STA-449C thermoanalyzer with a heating rate of 10°C/min under a nitrogen atmosphere. All fluorescence measurements were performed on an Edinburgh Instrument F920 spectrometer. UV/Vis absorption spectra were measured with a Hitachi UV-Vis spectrophotometer (Hitachi, Japan). X-ray photoelectron spectroscopy (XPS) experiments were performed using an Al Ka source, with an energy of 1486.6 eV at room temperature.

Synthesis of 4-carboxy-1-(4-carboxybenzyl)pyridinium chloride (H₂CcbpCl): A mixture of Isonicotinic acid (1.2311 g, 10 mmol) and Methyl 4-(bromomethyl)benzoate (2.2908 g, 10 mmol) in CH₃CN (50ml) was refluxed for 5h. After the mixture was cooled down to room temperature, the resulting precipitate was filtered to give white solid which was dissolved and refluxed in 100ml 2N HCl aqueous solution for 2h. After the solution cooled down to ambient temperature, the white precipitate formed were collected by filtration and washed with ether (20 ml \times 3) to afford H₂CcbpCl (3.14 g, 95%) which was identical to data in the literature.¹ ¹H NMR (400 Hz, DMSO-*d*6): δ = 9.53 (d, 2H, ArH, *J* = 6.0 Hz), 8.50 (d, 2H, ArH, *J* = 6.0 Hz), 7.96 (d, 2H, ArH, *J* = 8.0 Hz), 7.74 (d, 2H, ArH, *J* = 8.0 Hz), 6.18 (s, 2H, CH₂); ¹³C NMR (100 Hz, DMSO-*d*6): δ = 167.1, 163.8, 146.9, 146.4, 139.1, 132.0, 130.4, 129.6, 128.2, 63.1. (Fig. S1 and 2, ESI†) Main IR (KBr, cm⁻¹): 3411, 3058, 2668, 2549, 2397, 1703, 1392, 1242. (Fig. S3, ESI†)

Luminescence Measurements:

Before photoluminescence measurements, the suspensions were oscillated for 10 min using ultrasonic waves to ensure uniform dispersion.

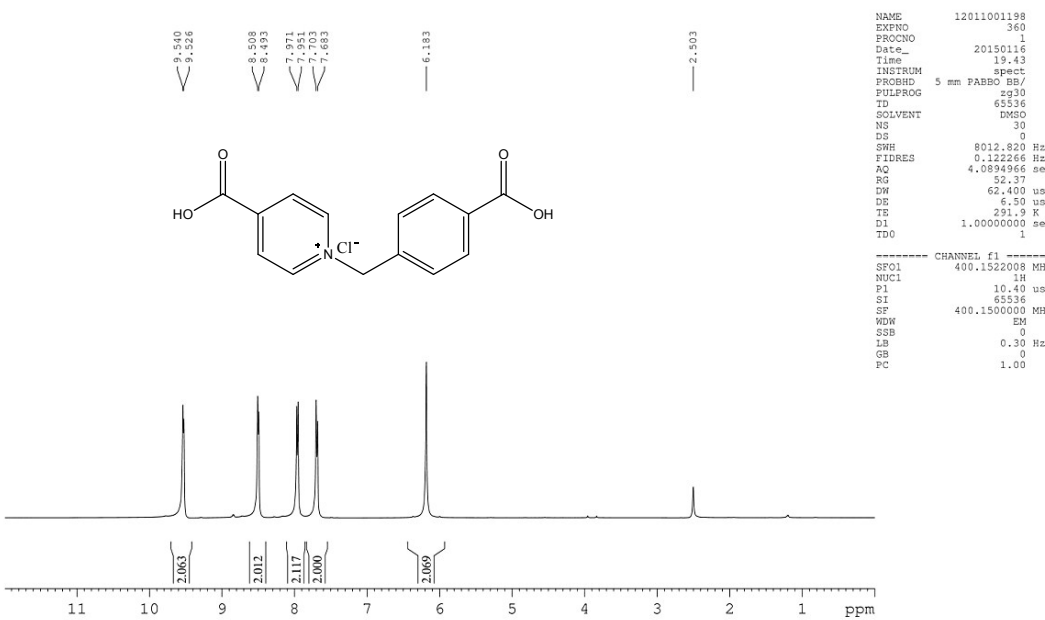


Figure S1. ^1H NMR (400 Hz, $\text{DMSO}-d_6$) spectra of ligand H_2CcbpCl

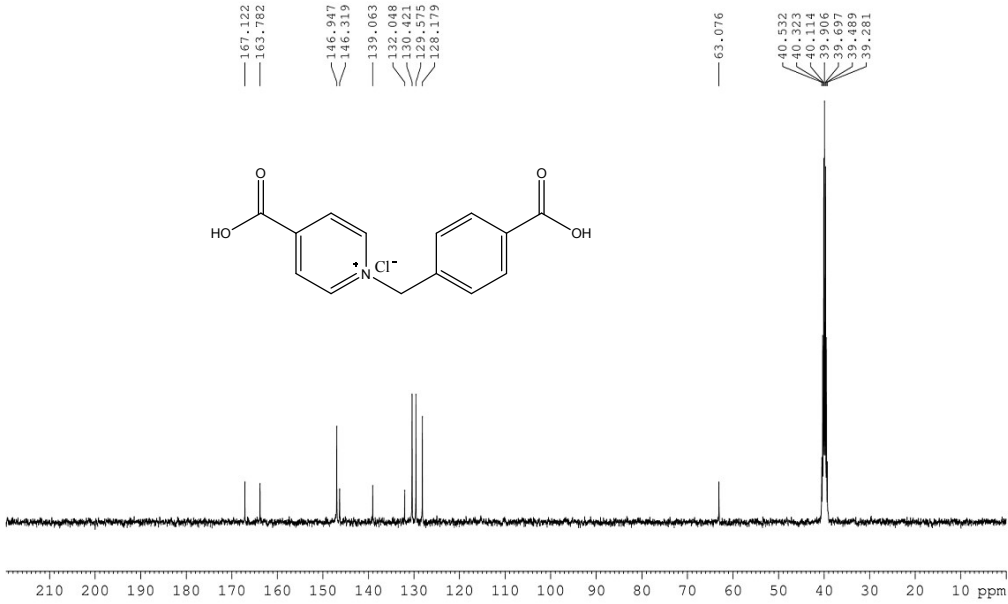


Figure S2. ^{13}C NMR (100 Hz, $\text{DMSO}-d_6$) spectra of ligand H_2CcbpCl

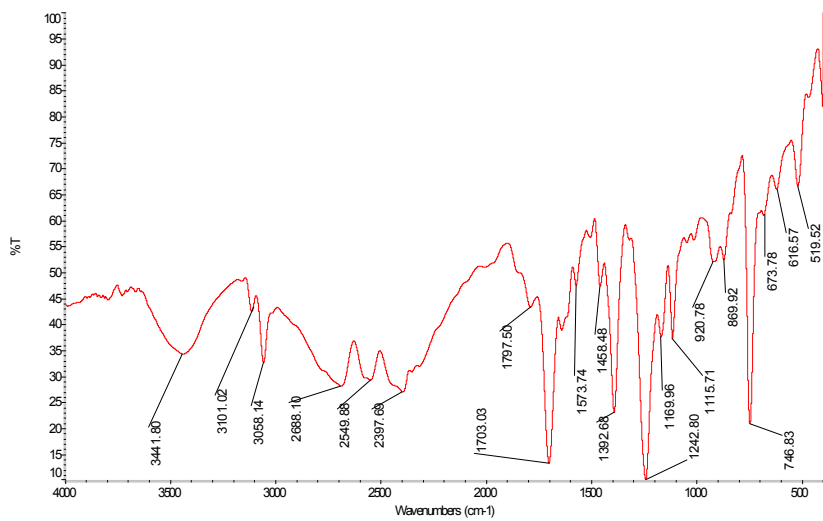


Figure S3. The IR spectra of ligand

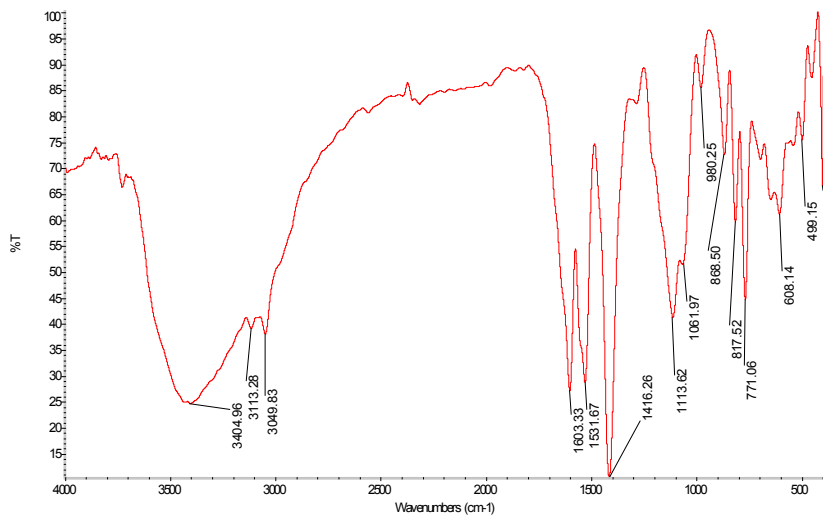


Figure S4. The IR spectra of Tb-MOF **1**

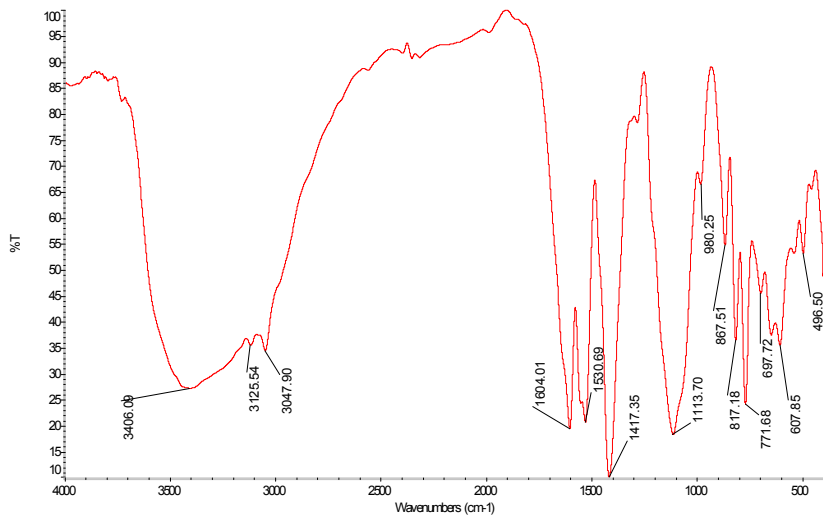


Figure S5. The IR spectra of Eu-MOF **2**

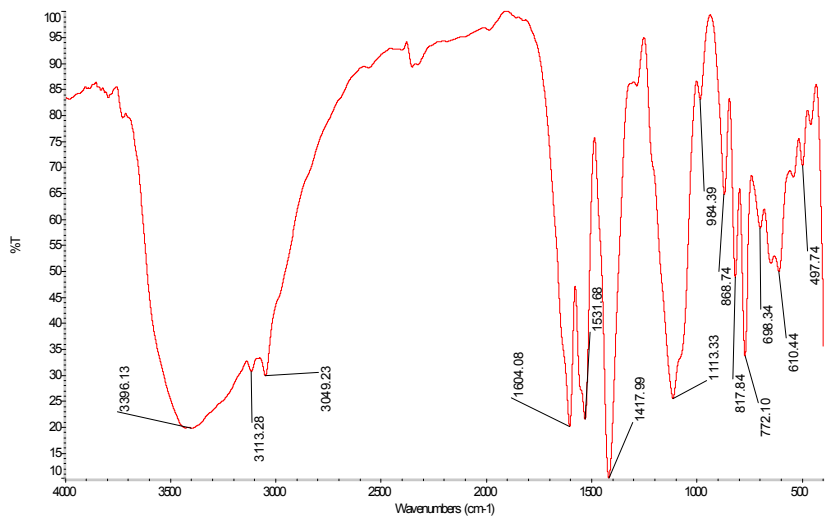


Figure S6. The IR spectra of Gd-MOF 3

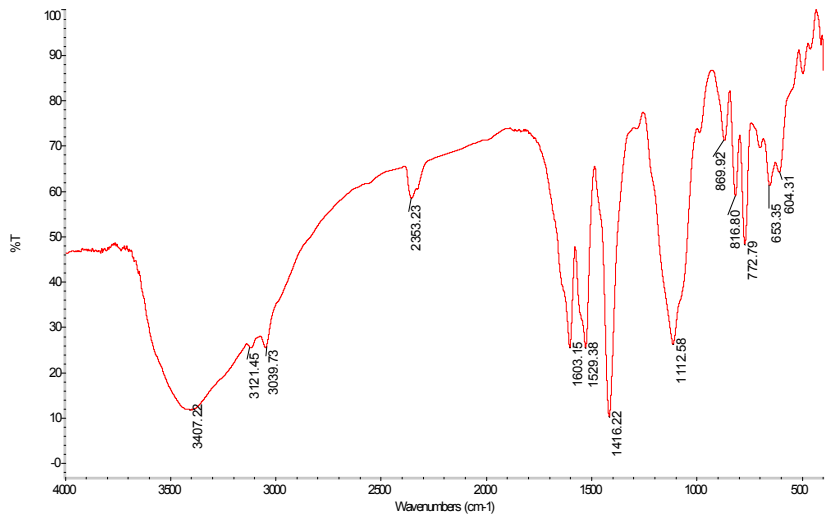


Figure S7. The IR spectra of Sm-MOF 4

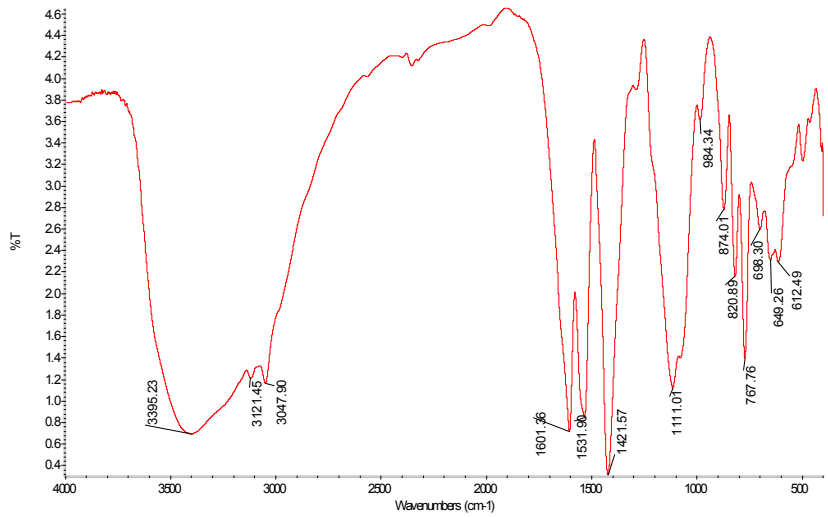


Figure S8. The IR spectra of Er-MOF 5

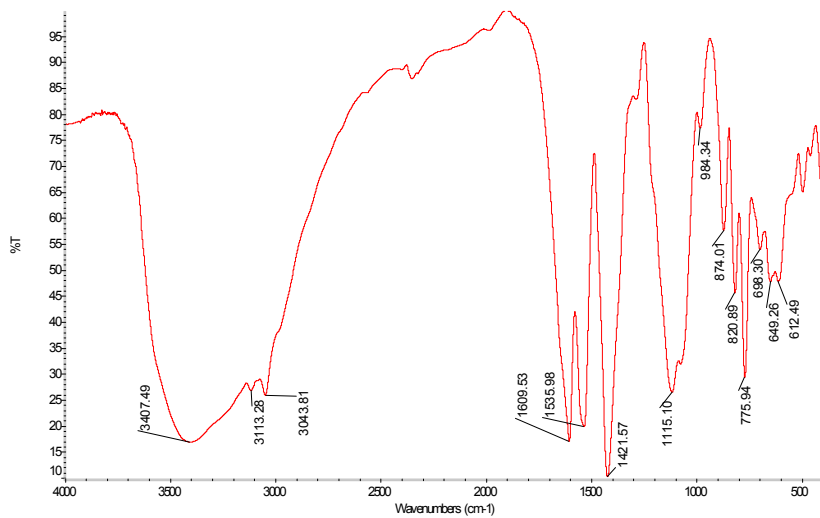


Figure S9. The IR spectra of Yb-MOF 6

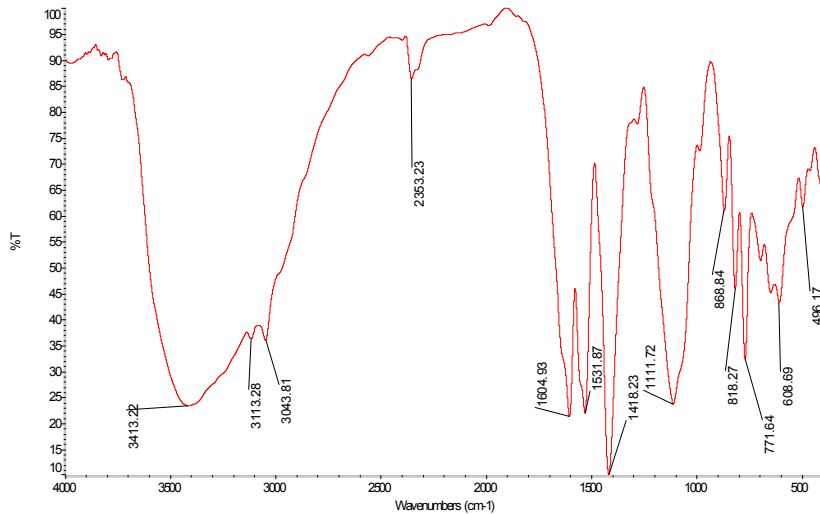


Figure S10. The IR spectra of Tb_{1.828}Eu_{0.172}-MOF 7

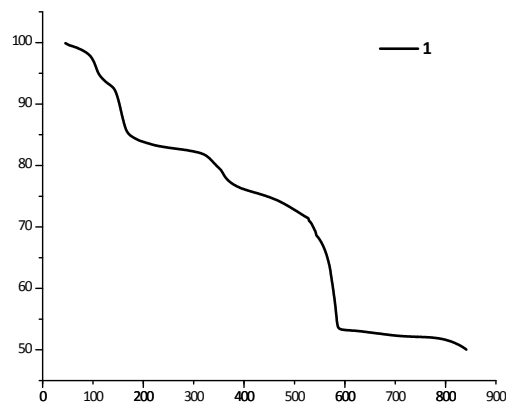


Figure S11. The TGA diagrams of Tb-MOF 1

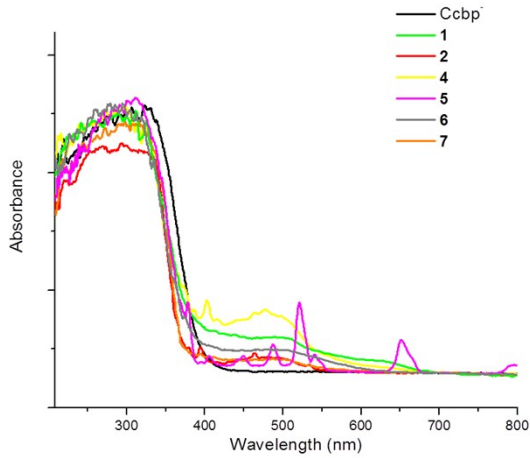


Figure S12. UV-vis absorption spectra of the ligand and MOFs **1-7**.

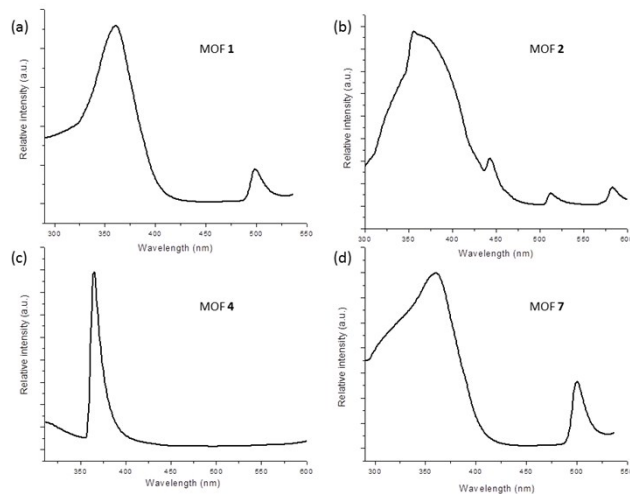


Figure S13. The solid-state excitation spectra of (a) MOF **1** with $\lambda_{\text{em}} = 543 \text{ nm}$, (b) MOF **2** with $\lambda_{\text{em}} = 613 \text{ nm}$, (c) MOF **4** with $\lambda_{\text{em}} = 599 \text{ nm}$, (d) MOF **7** with $\lambda_{\text{em}} = 543 \text{ nm}$.

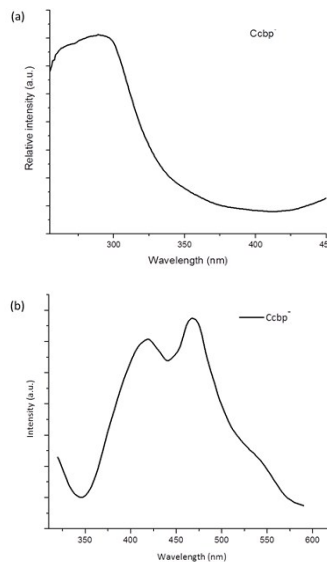


Figure S14. (a)The solid-state excitation spectra of ligand with $\lambda_{\text{em}} = 470 \text{ nm}$, (b) The solid-state emission spectra of ligand with $\lambda_{\text{ex}} = 302 \text{ nm}$.

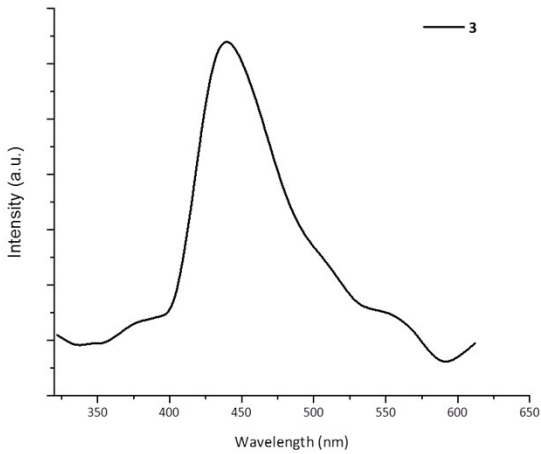


Figure S15. The phosphorescence spectra of the Gd-MOF **3** in the solid state at 77 K.

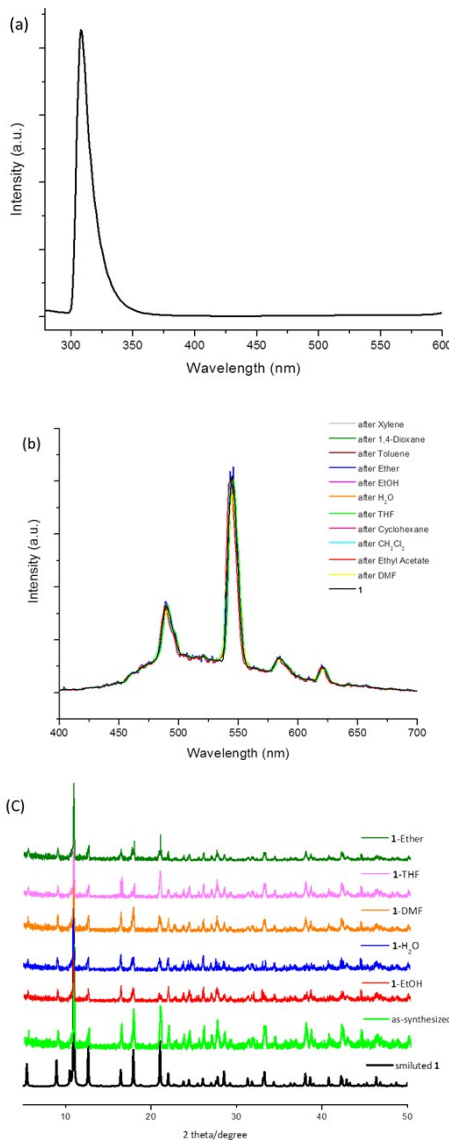


Figure S16. (a) The excitation spectra of MOF **1** in the solution of ethanol with $\lambda_{\text{em}} = 543 \text{ nm}$, (b) The solid-state emission spectra of ligand with $\lambda_{\text{ex}} = 360 \text{ nm}$ after the solvent sensing tests, (c) PXRD patterns of **1** after sensing some representative different solvent.

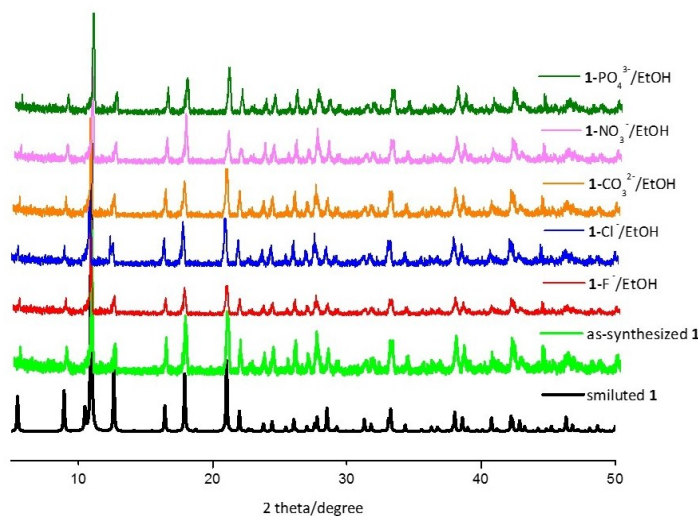


Figure S17. PXRD patterns of **1** after sensing some representative different anions.

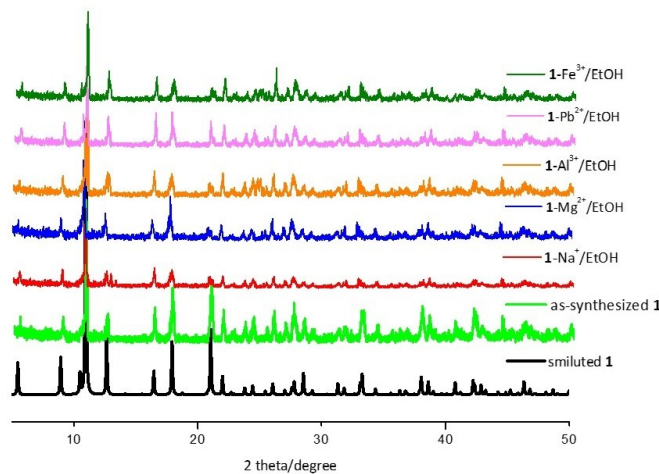


Figure S18. PXRD patterns of **1** after sensing some representative different cations

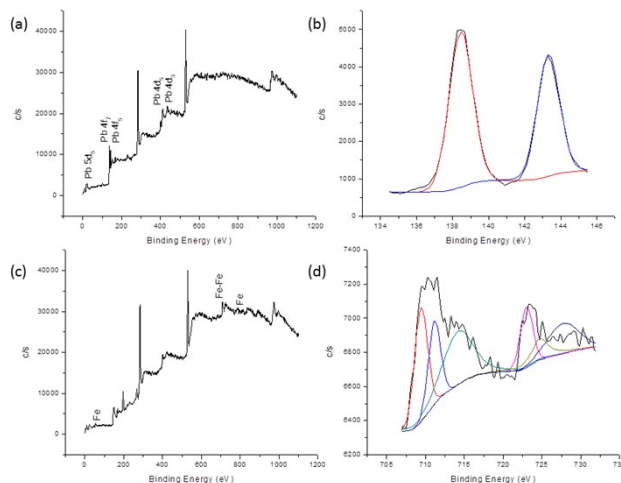


Figure S19. (a) and (b): the XPS for MOF **1** after interacting with Pb^{2+} , no obvious Pb (0) from 136.4 to 136.9 eV and Pb(iv) at 137.4 eV, while the peaks of Pb(ii) at 138.46 eV appears; (c) and (d): the XPS for MOF **1** after interacting with Fe^{3+} , no obvious Fe (ii) at 710.6, 712.1 and 710.3 eV, while the peaks of Fe(iii) at 711.3 eV appears.

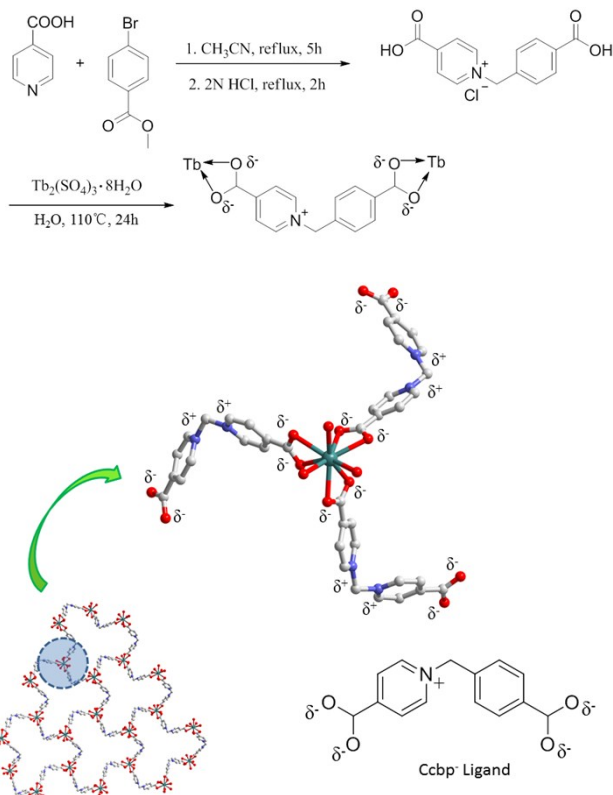


Figure S20. View of the regular charge distributions of MOF 1.

This work employed a zwitterionic pyridinium ligand Ccbp⁻ which molecule with a charge separated skeleton is thought to be polarized. Although the carboxylate oxygen atoms of the Ccbp⁻ ligand in MOF 1 all take part in the coordination with Tb³⁺, leaving no common active sites (COOH, etc.) for the effective interaction between metal ions and MOF 1, we have obtained a framework featuring well located charge distributions with one side decorated with positive charges (pyridinium cations) while another side has negative charges (carboxylate oxygens), which generates a regularly distributed electrostatic field and shows selective affinity for guest molecules.

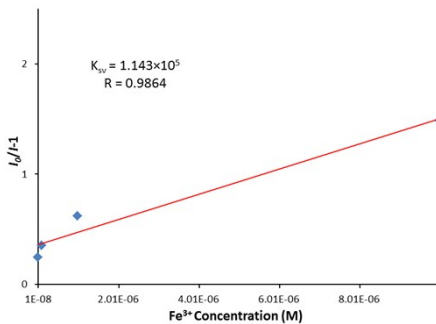


Figure S21. The Stern–Volmer plot of I_0/I versus the concentration of Fe³⁺ ions in the 1–ethanol suspension.

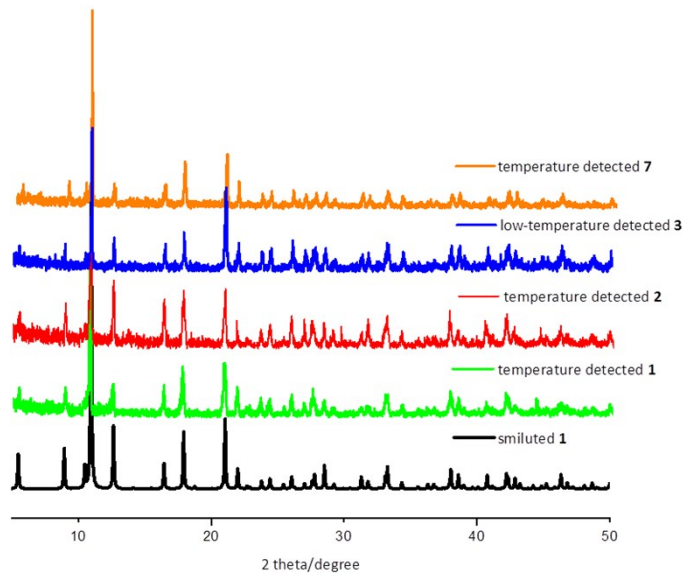


Figure S22. PXRD patterns of **1** after sensing the temperature from 10K to 300K.

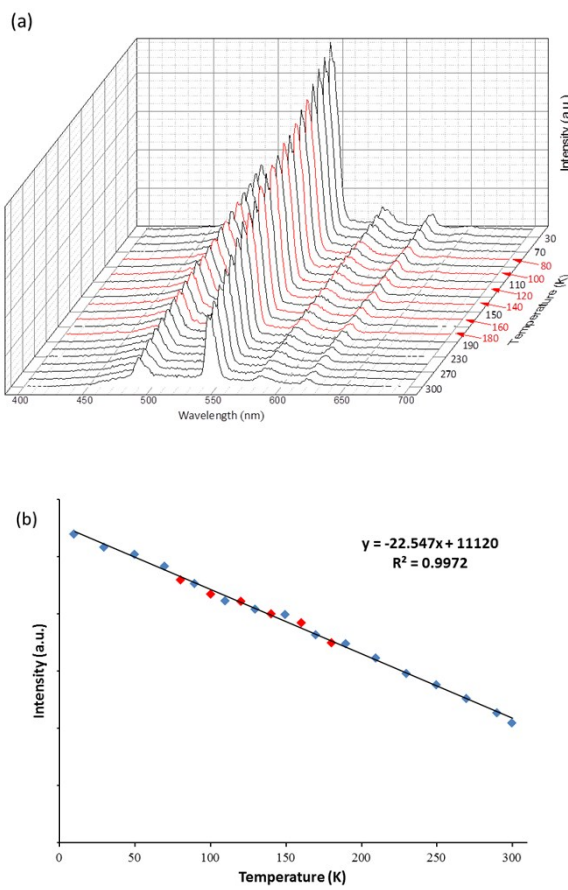


Figure S23. (a) The luminescence of the Tb-MOF **1** from 180 to 80 K, (b) view the luminescence has the same change with the decrease of temperature.

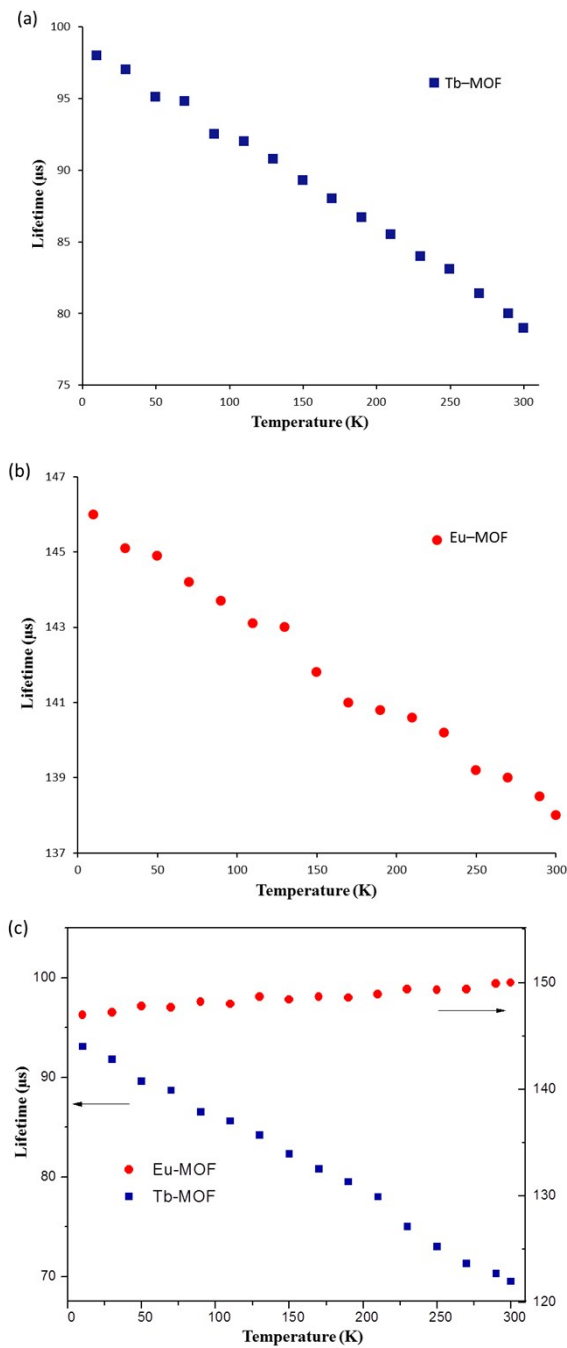


Figure S24. (a) Temperature dependent $5D_4$ lifetimes of **1** (543 nm) (10 – 300 K). The decay curves are monitored at 543 nm and excited at 360 nm, (b) Temperature dependent $5D_0$ lifetimes of **2** (613 nm) (10 – 300 K). The decay curves are monitored at 613 nm and excited at 360 nm, (c) Temperature dependent $5D_4$ and $5D_0$ lifetimes of the mixed MOF **7** (543 nm) (10 – 300 K). The decay curves are monitored at 543 and 613 nm, respectively, and excited at 360 nm.

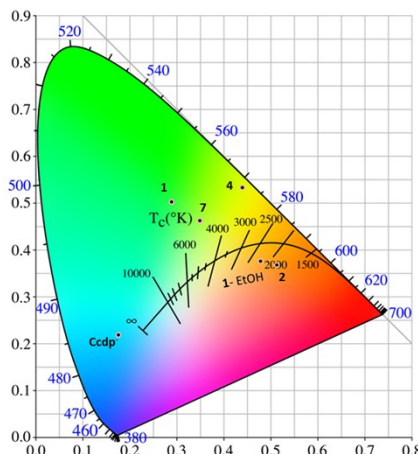


Figure S25. The CIE chromaticity diagram showing the Tb-MOF **1**, Eu-MOF **2**, Sm-MOF **4**, Tb+Eu MOF **7**, **1**-Ethanol and the free ligand Ccbp⁻.

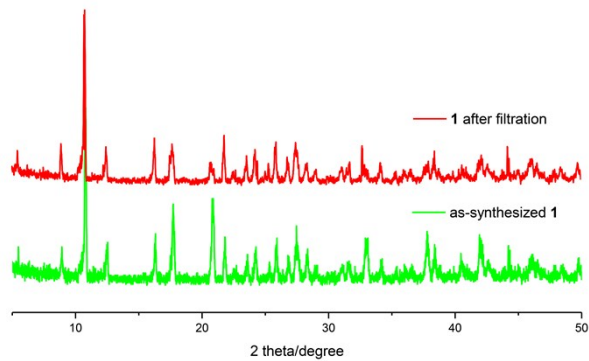


Figure S26. The PXRD of the MOF **1** (the residue) collected from filter of the **1**-dispersion.

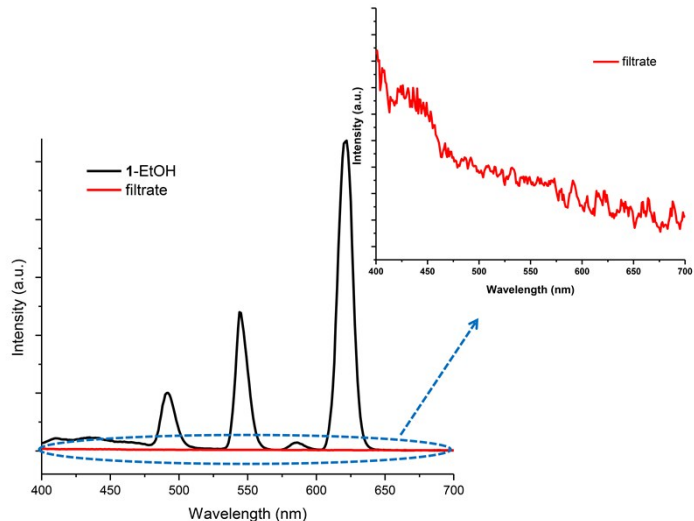


Figure S27. The luminescence of the filtrate filtered from the **1**-dispersion (red line, excited at 308nm) compared with the luminescence of the **1**-dispersion (black line, excited at 308nm). The insert is the enlarged view of The luminescence of the filtrate filtered from the **1**-dispersion (excited at 308nm).

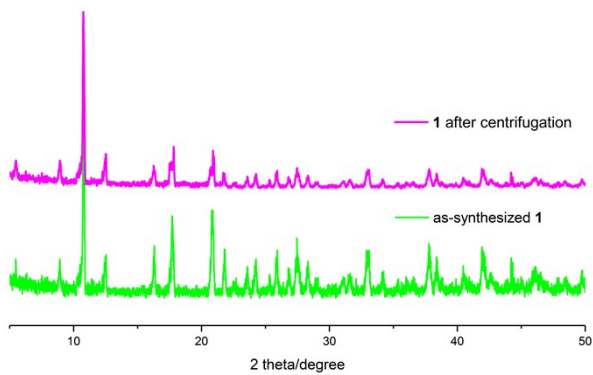


Figure S28. The PXRD of the solid MOF **1** by centrifugation of the **1**-dispersion.

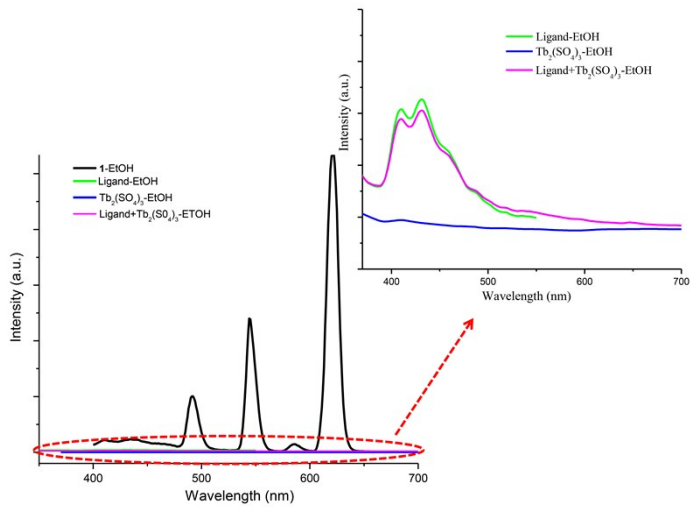


Figure S29. The luminescence of the $\text{Tb}_2(\text{SO}_4)_3$ dissolved in ethanol (blue line, excited at 308nm), the luminescence of the free H_2CcbpCl ligand dissolved in ethanol (green line, excited at 308nm) and the luminescence of the solution by $\text{Tb}_2(\text{SO}_4)_3/\text{free H}_2\text{CcbpCl}$ ligand (3:1) directly added to ethanol (pink line, excited at 308nm) compared with the luminescence of the **1**-dispersion (black line, excited at 308nm). The insert is the enlarged view of the luminescence of the above experiments.

Table S1 Elected bond lengths (\AA) and angles ($^\circ$) for compound **Tb-MOF 1**

O1—Tb1	2.453 (6)	Tb1—O2C	2.422 (6)
O2—Tb1	2.422 (6)	Tb1—O1C	2.453 (6)
O3—Tb1	2.390 (7)	Tb1—O1B	2.453 (6)
Tb1—O3C	2.390 (7)	C8—O1	1.278 (9)
Tb1—O3B	2.390 (7)	C7—N1A	1.495 (9)
Tb1—O2B	2.422 (6)	C7—C4A	1.495 (9)
O3B—Tb1—O1	77.7 (2)	O3C—Tb1—O3	77.9 (2)
O3—Tb1—O1	144.0 (2)	O3B—Tb1—O3	77.9 (2)
O2B—Tb1—O1	75.0 (2)	O3C—Tb1—O2B	91.7 (2)
O2C—Tb1—O1	124.0 (2)	O3B—Tb1—O2B	152.7 (2)
O2—Tb1—O1	53.60 (18)	O3—Tb1—O2B	125.0 (2)
O3C—Tb1—O1C	144.0 (2)	O3C—Tb1—O2C	152.7 (2)
O3B—Tb1—O1C	71.5 (2)	O3B—Tb1—O2C	125.0 (2)
O3—Tb1—O1C	77.7 (2)	O3—Tb1—O2C	91.7 (2)
O2B—Tb1—O1C	124.05 (19)	O2B—Tb1—O2C	73.6 (2)
O2C—Tb1—O1C	53.60 (18)	O3C—Tb1—O2	125.0 (2)
O2—Tb1—O1C	75.0 (2)	O3B—Tb1—O2	91.7 (2)
O1—Tb1—O1C	118.20 (6)	O3—Tb1—O2	152.7 (2)
O3C—Tb1—O1B	77.7 (2)	O2B—Tb1—O2	73.6 (2)
O3B—Tb1—O1B	144.0 (2)	O2C—Tb1—O2	73.6 (2)
O3—Tb1—O1B	71.5 (2)	O3C—Tb1—O1	71.5 (2)
O2B—Tb1—O1B	53.60 (18)	O2—C8—O1	119.3 (7)
O2C—Tb1—O1B	75.0 (2)	O2—C8—C1	122.4 (7)
O2—Tb1—O1B	124.0 (2)	O1—C8—C1	118.3 (7)
O1—Tb1—O1B	118.20 (6)	O2—C8—Tb1	59.0 (4)
O1C—Tb1—O1B	118.20 (6)	O1—C8—Tb1	60.4 (4)
O3C—Tb1—O3B	77.9 (2)		
C6—C1—C2—C3	-1.6 (13)	C5—C4—C7—N1A	-134.5 (7)
C8—C1—C2—C3	177.4 (8)	C3—C4—C7—C4A	46.8 (7)
C1—C2—C3—C4	-0.4 (14)	C5—C4—C7—C4A	-134.5 (7)
C2—C3—C4—C5	-0.3 (14)	C6—C1—C8—O2	162.1 (8)
C2—C3—C4—C7	178.4 (8)	C2—C1—C8—O2	-16.9 (11)
C6—C5—C4—C3	3.1 (12)	C6—C1—C8—O1	-20.3 (11)
C6—C5—C4—C7	-175.6 (7)	C2—C1—C8—O1	160.8 (7)
C4—C5—C6—C1	-5.2 (12)	O2—C8—O1—Tb1	3.7 (7)
C2—C1—C6—C5	4.4 (12)	C1—C8—O1—Tb1	-174.0 (6)
C8—C1—C6—C5	-174.6 (7)	O1—C8—O2—Tb1	-3.8 (8)
C3—C4—C7—N1A	46.8 (7)	C1—C8—O2—Tb1	173.9 (6)

Symmetry codes: (A) $-x+3/4, z-1/4, y+1/4$; (C) $z-1/2, -x+1/2, -y+1$; (B) $-y+1/2, -z+1, x+1/2$.

Table S2 Elected bond lengths (\AA) and angles ($^\circ$) for compound **Gd-MOF 3**

Gd1—O3B	2.426 (7)	C7—N1	1.498 (10)
Gd1—O3A	2.426 (7)	C7—N1C	1.498 (10)
Gd1—O3	2.426 (7)	C7—C4C	1.498 (10)
Gd1—O1	2.465 (6)	C8—O1	1.255 (10)
Gd1—O1B	2.465 (6)	C8—O2	1.286 (10)
Gd1—O1A	2.465 (6)	C3—N1	1.363 (12)
Gd1—O2	2.471 (6)	C1—C6	1.396 (11)
Gd1—O2A	2.471 (6)	C1—C2	1.433 (12)
Gd1—O2B	2.471 (6)	C1—C8	1.476 (12)
O1A—Gd1—O2	123.9 (2)	O3A—Gd1—O2B	77.9 (2)
O3B—Gd1—O2A	71.6 (2)	O3—Gd1—O2B	71.6 (2)
O3A—Gd1—O2A	144.2 (2)	O1—Gd1—O2B	123.9 (2)
O3—Gd1—O2A	77.9 (2)	O1B—Gd1—O2B	53.12 (18)
O1—Gd1—O2A	75.1 (2)	O1A—Gd1—O2B	75.1 (2)
O1B—Gd1—O2A	123.9 (2)	O2—Gd1—O2B	118.12 (6)
O1A—Gd1—O2A	53.12 (18)	O2A—Gd1—O2B	118.11 (6)
O3B—Gd1—O2B	144.2 (2)	O3B—Gd1—C8A	98.5 (2)
O3B—Gd1—O3A	77.8 (3)	O3B—Gd1—O1A	124.7 (2)
O3B—Gd1—O3	77.8 (3)	O3A—Gd1—O1A	152.9 (2)
O3A—Gd1—O3	77.8 (3)	O3—Gd1—O1A	91.6 (2)
O3B—Gd1—O1	91.6 (2)	O1—Gd1—O1A	73.9 (2)
O3A—Gd1—O1	124.7 (2)	O1B—Gd1—O1A	73.9 (2)
O3—Gd1—O1	152.9 (2)	O3B—Gd1—O2	77.9 (2)
O3B—Gd1—O1B	152.9 (2)	O3A—Gd1—O2	71.6 (2)
O3A—Gd1—O1B	91.6 (2)	O3—Gd1—O2	144.2 (2)
O3—Gd1—O1B	124.7 (2)	O1—Gd1—O2	53.12 (18)
O1—Gd1—O1B	73.9 (2)	O1B—Gd1—O2	75.1 (2)
O1—C8—O2	120.5 (8)	N1—C7—N1C	112.8 (10)
O1—C8—C1	121.4 (8)	C4—C7—C4C	112.8 (10)
O2—C8—C1	118.0 (8)		
C6—C1—C2—C3	4.0 (14)	C2—C1—C8—O2	-159.2 (8)
C8—C1—C2—C3	-176.6 (9)	C2—C3—N1—C5	2.5 (15)

C1—C2—C3—N1	-2.6 (15)	C2—C3—N1—C7	-178.6 (9)
C1—C2—C3—C4	-2.6 (15)	C6—C5—N1—C3	-3.7 (13)
C2—C3—C4—C5	2.5 (15)	C6—C5—N1—C7	177.3 (7)
C2—C3—C4—C7	-178.6 (9)	N1C—C7—N1—C3	-45.7 (7)
C3—C4—C5—C6	-3.7 (13)	N1C—C7—N1—C5	133.2 (8)
C7—C4—C5—C6	177.3 (7)	O2—C8—O1—Gd1	3.4 (8)
N1—C5—C6—C1	5.2 (13)	C1—C8—O1—Gd1	-173.6 (7)
C4—C5—C6—C1	5.2 (13)	O1—C8—O2—Gd1	-3.4 (8)
C2—C1—C6—C5	-5.3 (13)	C1—C8—O2—Gd1	173.7 (6)

Symmetry codes: (A) -z+1, -x+1, y; (B) -y+1, z, -x+1; (C) y+3/4, x-3/4, -z-1/4.

Table S3 Elected bond lengths (\AA) and angles ($^\circ$) for compound **Sm-MOF 4**

Sm1—O3A	2.438 (9)	Sm1—O1	2.501 (8)
Sm1—O3B	2.438 (9)	Sm1—O1B	2.501 (8)
Sm1—O3	2.438 (9)	Sm1—O1A	2.501 (8)
Sm1—O2	2.488 (8)	O1—C8	1.253 (12)
Sm1—O2A	2.488 (8)	O2—C8	1.272 (12)
Sm1—O2B	2.488 (8)	C3—N1	1.361 (15)
O3A—Sm1—O3B	78.1 (3)	O2—Sm1—O1B	74.9 (3)
O3A—Sm1—O3	78.1 (3)	O2A—Sm1—O1B	123.8 (3)
O3B—Sm1—O3	78.1 (3)	O2B—Sm1—O1B	52.4 (2)
O3A—Sm1—O2	153.4 (3)	O1—Sm1—O1B	117.89 (8)
O3B—Sm1—O2	91.2 (3)	O3A—Sm1—O1A	71.5 (3)
O3—Sm1—O2	123.8 (3)	O3B—Sm1—O1A	144.8 (3)
O3A—Sm1—O2A	123.8 (3)	O3—Sm1—O1A	78.6 (3)
O3B—Sm1—O2A	153.4 (3)	O2—Sm1—O1A	123.8 (3)
O3—Sm1—O2A	91.2 (3)	O2A—Sm1—O1A	52.4 (2)
O2—Sm1—O2A	74.5 (3)	O2B—Sm1—O1A	74.9 (3)
O3A—Sm1—O2B	91.2 (3)	O1—Sm1—O1A	117.89 (8)
O3B—Sm1—O2B	123.8 (3)	O1B—Sm1—O1A	117.89 (8)
O3—Sm1—O2B	153.4 (3)	O3—Sm1—O1A	78.6 (3)
O2—Sm1—O2B	74.5 (3)	C5—C4—C7	119.3 (9)
O2A—Sm1—O2B	74.4 (3)	C3—N1—C5	117.6 (10)
O3A—Sm1—O1	144.8 (3)	C3—N1—C7	123.1 (10)
O3B—Sm1—O1	78.6 (3)	C5—N1—C7	119.3 (9)
O3—Sm1—O1	71.5 (3)	C6—C5—C4	121.2 (9)
O2—Sm1—O1	52.4 (2)	O1—C8—C1	118.1 (9)
O2A—Sm1—O1	74.9 (3)	O2—C8—C1	120.4 (9)
O2B—Sm1—O1	123.8 (3)	O1—C8—Sm1	61.0 (6)
O3A—Sm1—O1B	78.6 (3)	O2—C8—Sm1	60.5 (5)
O3B—Sm1—O1B	71.5 (3)	C1—C8—Sm1	174.5 (7)
O3—Sm1—O1B	144.8 (3)		
C1—C2—C3—C4	-1 (2)	C5—C4—C7—C4C	133.4 (10)

C2—C3—C4—C5	0.4 (19)	C3—N1—C7—N1C	-47.3 (10)
C2—C3—C4—C7	-179.0 (12)	C5—N1—C7—N1C	133.4 (10)
C2—C3—N1—C5	0.4 (19)	Sm1—O1—C8—O2	-3.4 (10)
C2—C3—N1—C7	-179.0 (12)	Sm1—O1—C8—C1	173.8 (7)
C3—C4—C5—C6	-2.0 (16)	Sm1—O2—C8—O1	3.4 (11)
C7—C4—C5—C6	177.4 (9)	Sm1—O2—C8—C1	-173.7 (8)
C3—N1—C5—C6	-2.0 (16)	C6—C1—C8—O1	20.8 (14)
C7—N1—C5—C6	177.4 (9)	C2—C1—C8—O1	-158.6 (10)
C8—C1—C6—C5	175.8 (9)	C2—C1—C8—O2	18.6 (14)

Symmetry codes: (A) $-z+1/2, -x+1/2, y$; (B) $-y+1/2, z, -x+1/2$; (C) $z+1/4, -y+3/4, x-1/4$; (D) $-y+3/4, -x+3/4, -z+1/4$.

Table S4 Selected bond lengths (\AA) and angles ($^\circ$) for compound **Er-MOF 5**

Er1—O3	2.362 (6)	C4—C5	1.355 (10)
Er1—O3C	2.362 (6)	C4—C9	1.506 (8)
Er1—O3B	2.362 (6)	N1—C5	1.355 (10)
Er1—O2	2.411 (5)	N1—C9	1.506 (8)
Er1—O2C	2.411 (5)	C5—C6	1.390 (12)
Er1—O2B	2.411 (5)	C7—O1	1.269 (8)
Er1—O1C	2.423 (5)	C7—O2	1.272 (9)
Er1—O1B	2.423 (5)	C9—N1A	1.506 (8)
Er1—O1	2.423 (5)	C9—C4A	1.506 (8)
O3—Er1—O1B	71.37 (18)	O3—Er1—O2	91.16 (19)
O3C—Er1—O1B	143.97 (18)	O3C—Er1—O2	125.47 (19)
O3B—Er1—O1B	77.10 (19)	O3B—Er1—O2	151.8 (2)
O2—Er1—O1B	74.79 (18)	O3—Er1—O2C	151.8 (2)
O2C—Er1—O1B	124.61 (17)	O3C—Er1—O2C	91.2 (2)
O2B—Er1—O1B	54.16 (16)	O3B—Er1—O2C	125.47 (19)
O1C—Er1—O1B	118.35 (5)	O2—Er1—O2C	73.8 (2)
O3—Er1—O1	77.10 (19)	O3—Er1—O2B	125.47 (19)
O3C—Er1—O1	71.38 (18)	O3C—Er1—O2B	151.8 (2)
O3B—Er1—O1	143.97 (18)	O3B—Er1—O2B	91.16 (19)
O2—Er1—O1	54.16 (16)	O2—Er1—O2B	73.8 (2)
O2C—Er1—O1	74.79 (18)	O2C—Er1—O2B	73.8 (2)
O2B—Er1—O1	124.61 (17)	O3—Er1—O1C	143.97 (18)
O1C—Er1—O1	118.35 (5)	O3C—Er1—O1C	77.10 (19)
O1B—Er1—O1	118.35 (5)	O3B—Er1—O1C	71.38 (18)
O3—Er1—O3C	78.2 (2)	O2—Er1—O1C	124.61 (17)
O3—Er1—O3B	78.2 (2)	O2C—Er1—O1C	54.16 (16)
O3C—Er1—O3B	78.2 (2)	O2B—Er1—O1C	74.79 (18)
C1—C2—C3—C4	-0.5 (13)	C2—C1—C7—O1	160.0 (7)
C2—C3—C4—C5	2.0 (13)	C6—C1—C7—O2	162.0 (7)
C2—C3—C4—C9	178.0 (7)	C2—C1—C7—O2	-17.5 (10)

C2—C3—N1—C5	2.0 (13)	C5—C4—C9—C4A	-135.9 (7)
C2—C3—N1—C9	178.0 (7)	C3—C4—C9—C4A	48.0 (6)
C3—N1—C5—C6	0.1 (11)	C5—N1—C9—N1A	-135.9 (7)
C9—N1—C5—C6	-176.0 (6)	C3—N1—C9—N1A	48.0 (6)
C3—C4—C5—C6	0.1 (11)	O2—C7—O1—Er1	4.5 (7)
C9—C4—C5—C6	-176.0 (6)	C1—C7—O1—Er1	-173.1 (5)
C2—C1—C6—C5	4.9 (11)	O1—C7—O2—Er1	-4.5 (7)
C7—C1—C6—C5	-174.6 (6)	C1—C7—O2—Er1	173.1 (6)

Symmetry codes: (A) $z-1/4, -y+7/4, x+1/4$; (C) $y-1/2, -z+1, -x+1/2$; (B) $-z+1/2, x+1/2, -y+1$; (D) $-y+1, z+1/2, -x+1/2$; (E) $-z+1/2, -x+1, y-1/2$.

Table S5 Elected bond lengths (\AA) and angles ($^\circ$) for compound **Yb-MOF 6**

Yb1—O3B	2.338 (11)	O1—Yb1	2.420 (11)
Yb1—O3C	2.338 (11)	O4—O4C	1.12 (7)
Yb1—O2B	2.379 (10)	O4—O4B	1.12 (7)
Yb1—O2C	2.379 (10)	C8—O2	1.276 (19)
Yb1—O1B	2.420 (11)	C8—O1	1.294 (17)
Yb1—O1C	2.420 (11)	C10—N1	1.488 (17)
Yb1—O3B	2.338 (11)		
O3C—Yb1—O1B	143.4 (4)	C8—O1—Yb1	91.6 (10)
O3—Yb1—O1B	77.3 (4)	O3B—Yb1—O3C	77.7 (4)
O2B—Yb1—O1B	55.0 (4)	O3B—Yb1—O3	77.7 (4)
O2C—Yb1—O1B	73.8 (4)	O3C—Yb1—O3	77.7 (4)
O2—Yb1—O1B	125.8 (4)	O3B—Yb1—O2B	126.2 (4)
O3B—Yb1—O1C	77.3 (4)	O3C—Yb1—O2B	150.9 (5)
O3C—Yb1—O1C	71.2 (4)	O3—Yb1—O2B	90.6 (4)
O3—Yb1—O1C	143.4 (4)	O3B—Yb1—O2C	90.6 (4)
O2B—Yb1—O1C	125.8 (4)	O3C—Yb1—O2C	126.2 (4)
O2C—Yb1—O1C	55.0 (4)	O3—Yb1—O2C	150.9 (5)
O2—Yb1—O1C	73.8 (4)	O2B—Yb1—O2C	74.7 (4)
O1B—Yb1—O1C	118.44 (10)	O3B—Yb1—O2	150.9 (5)
O3B—Yb1—O1	143.4 (4)	O3C—Yb1—O2	90.7 (4)
O3C—Yb1—O1	77.3 (4)	O3—Yb1—O2	126.2 (4)
O3—Yb1—O1	71.2 (4)	O2B—Yb1—O2	74.7 (4)
O2B—Yb1—O1	73.8 (4)	O2C—Yb1—O2	74.7 (4)
O2C—Yb1—O1	125.8 (4)	O3B—Yb1—O1B	71.2 (4)
O2—Yb1—O1	55.0 (4)	C1—N1—C6	120.5 (14)
O1B—Yb1—O1	118.44 (10)	C1—N1—C10	119.0 (12)
O1C—Yb1—O1	118.45 (10)	C6—N1—C10	120.5 (13)
C7—C6—N1	119.2 (15)	O2—C8—O1	119.1 (14)
C8—C5—C7—C6	-176.7 (14)	C7—C6—N1—C10	-177.4 (13)

C12—C5—C8—O2	−160.9 (15)	N1A—C10—N1—C1	135.1 (14)
C7—C5—C8—O2	22 (2)	N1A—C10—N1—C6	−46.1 (12)
C12—C5—C8—O1	18 (2)	N1—C1—C12—C5	4 (2)
C7—C5—C8—O1	−158.6 (15)	C11—C1—C12—C5	4 (2)
C12—C1—C11—C6	−2 (2)	C7—C5—C12—C1	−7 (2)
C12—C1—C11—C10	177.0 (12)	C8—C5—C12—C1	176.4 (13)
C7—C6—C11—C1	1 (2)	O1—C8—O2—Yb1	5.9 (15)
C7—C6—C11—C10	−177.4 (13)	C5—C8—O2—Yb1	−174.8 (12)
C11A—C10—C11—C1	135.1 (14)	O2—C8—O1—Yb1	−5.8 (15)
C11A—C10—C11—C6	−46.1 (12)	C5—C8—O1—Yb1	174.9 (11)

Symmetry codes: (A) $-x+9/4, -z+5/4, -y+5/4$; (B) $y+1/2, z-1/2, x$; (C) $z, x-1/2, y+1/2$.

References

- (a) J.-Y. Zhang, K. Wang, X.-B. Li and E.-Q. Gao, *Inorg. Chem.*, 2014, **53**, 9306; (b) M. Chen, M.-Z. Chen, C.-Q. Zhou, W.-E. Lin, J.-X. Chen, W.-H. Chen and Z.-H. Jiang, *Inorg. Chim. Acta*, 2013, **405**, 461